2.2 Fine Scale Structure of a Squall Line Observed by the NCAR ELDORA

Wen-Chau Lee[#] Roger M. Wakimoto[*] John F. Gamache[%]

[#]National Center for Atmospheric Research[1], Boulder CO, 80307
[*]University of California, at Los Angeles, Los Angeles, CA 90095
[%]NOAA/AOML/Hurricane Research Division, Miami, FL 33149

1. Introduction

An intense squall line developed on 7 May 1995 in the Texas panhandle during VORTEX-95. Based on the Amarillo WSR-88D Doppler radar data (not shown), this north-south oriented squall line formed southeast of Amarillo, TX, along a cold front, moved into Oklahoma. Figure 1 illustrates the surface winds and θe at 1500 UTC (all times hereafter are UTC) superimposed on visible satellite image in the VORTEX domain. High θ_e By 2100, this squall line was about 600 km long and 100 km wide. The central part of the squall line was distorted into a bow echo after 2100 UTC and produced straight-line damage winds near Willow, OK.

Both the NCAR Electra and NOAA P-3 flew 40 km legs on the eastern side of this squall line at two different altitudes. ELDORA collected 300 m along track resolution data from 2013 to 2120 UTC (a total of 9 flight legs) with a data gap between 2055 to 2108 UTC. With additional data sources from the Amarillo WSR-88D data and surface measurements from NSSL ground team, the evolution and fine scale structure of this squall line segment and its accompanied mesocyclone were documented over a two-hour period.

The purpose of this paper is to present the evolution and fine scale structure of this squall line using primarily the dual-Doppler radar analyses from the NCAR ELDORA data. ELDORA's 300 m along track resolution resolved features with a wavelength of 2 km. The Doppler radar data were edited in the NCAR SOLO package (Oye et al. 1995). The Doppler radar data were interpolated using Barnes scheme with grid spacing of 500 m in all three dimensions. The wind fields are deduced using a 3-D variational Doppler analysis technique (Gamache 1997) where the continuity equation is included in the cost function so the vertical velocity is deduced simultaneously with horizontal velocities. This approach allows the retrieval of 3-D winds above 45° elevation angle.

2. Squall Line Structure

The evolution of the squall line over a 50-minute period is illustrated in Fig. 2. This squall line exhibited a complex structure that has not been documented in previous observational studies. A distinct mesocyclone and a hook echo were identified (12, 5) within this squall line at 2013 but no tornado was reported. An E-W vertical cross-section just south of the mesocyclone is shown in Fig. 3. The storm top reached 16 km AGL at this time. An updraft exceeding 20 m/s is co-located with the vault (near X=15 km). The high reflectivity east of the vault is accompanied by downdraft and formed a horizontal vortex circulation. The airflow diverged near the storm top and fed into the anvil in front of the squall line. The flight legs were centered on the mesocyclone after 2021. The NCAR Electra nearly flew into the mesoclone at 2025 and touched the 50 dBZ echo. This mistake, fortunately, resulted in direct observations of the weak echo vault above the aircraft by ELDORA (Fig. 4). Strong horizontal convergence was located near the leading edge of the squall line (X=18 km) where the Electra flew beneath the vault at 1 km altitude.

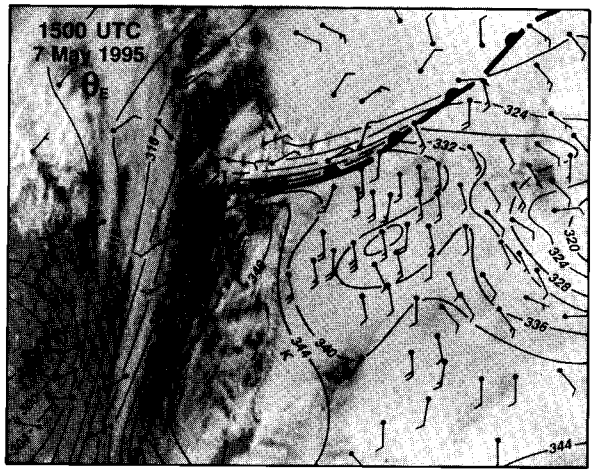

Figure 1: The surface winds and θ_e superimposed on the visible satellite image at 1500 7 May 1995.

The storm-relative environmental flow (hereafter all winds are storm-relative unless specified otherwise) funneled into the mesocyclone (Fig. 1). The bulge and kink of the squall line are consistent with the winds suggesting that the line echo wave pattern (LEWP) of the echo (at 2035) was produced by the mesocyclone circulation. The airflow north and south of the mesocyclone was quite different. The convergence line south of the mesocyclone was located near the leading edge of the squall line. However, the convergence line bent to the back of the storm north of the mesocyclone. This feature can also be illustrated in Fig. 5 with E-W vertical cross-sections on south (top panel) and north (bottom panel) of the mesocyclone. The convergence and updraft are located at the leading edge of the squall line south of the mesocyclone. A deep

[1]Corresponding author address: Wen-Chau Lee, NCAR Remote Sensing Facility, Boulder, CO 80307. NCAR is sponsored by the National Science Foundation.

convergence layer (up to 5 km) was resolved. The re-circulation of the main updraft is clearly shown. The echo overhang shown here was commonly observed during VORTEX-95 and has been proposed as one mechanism to form hail (e.g., Browning and Foote1976). The structure north of the mesocyclone exhibited quite different characteristics. The convergence was relatively shallow and was located deep into the line. The primary updraft and the active convection were behind the high reflectivity feature in the ELDORA data. This is probably due to attenuation of the 3-cm radar passing through heavy precipitation in the leading edge of the line. The high reflectivity in the mid and upper levels was associated with downdraft and falling precipitation. The differences in the vertical structures (e.g., sloping of the updraft) in different part of a squall line have been simulated in numerical model (Weisman and Davis 1998).

The peak updraft in upper atmosphere exceeds 60 m/s which is consistent with the CAPE exceeding 3000. Multiple horizontal vortex tubes (Doppler velocity dipoles in RHI scans) with speed exceeding 30 m/s were clearly seen along the interface between the receding flow (inflow) and approaching flow (outflow). An example is illustrated in Fig. 5. Similar horizontal vortex tubes also existed on the front end of the updraft vault associated with curling reflectivity factor.

The town Willow, OK is located near the apex (18,15) of the LEWP at 2049 (Fig. 1). It can be seen that the mesocyclone intensified between 2043 and 2049. A southerly wind exceeds 25 m/s is retrieved on the east side of the mesocyclone. The mesocyclone is moving at a speed of u=10.5 m/s and v=19.1 m/s. As a result, the ground-relative winds on the east side of the mesocyclone exceeded 45 m/s from the south that is consistent with most of the damage patterns reported surrounding Willow. The asymmetric enhancement of the ground-relative wind within the mesocyclone by its fast translation speed may be the reason for the straight-line damage pattern rather than a tornado like damage pattern.

The asymmetric enhancement of the ground-relative wind within the mesocyclone by its fast translation speed may be the reason for the straight-line damage pattern rather than a tornado like damage pattern.

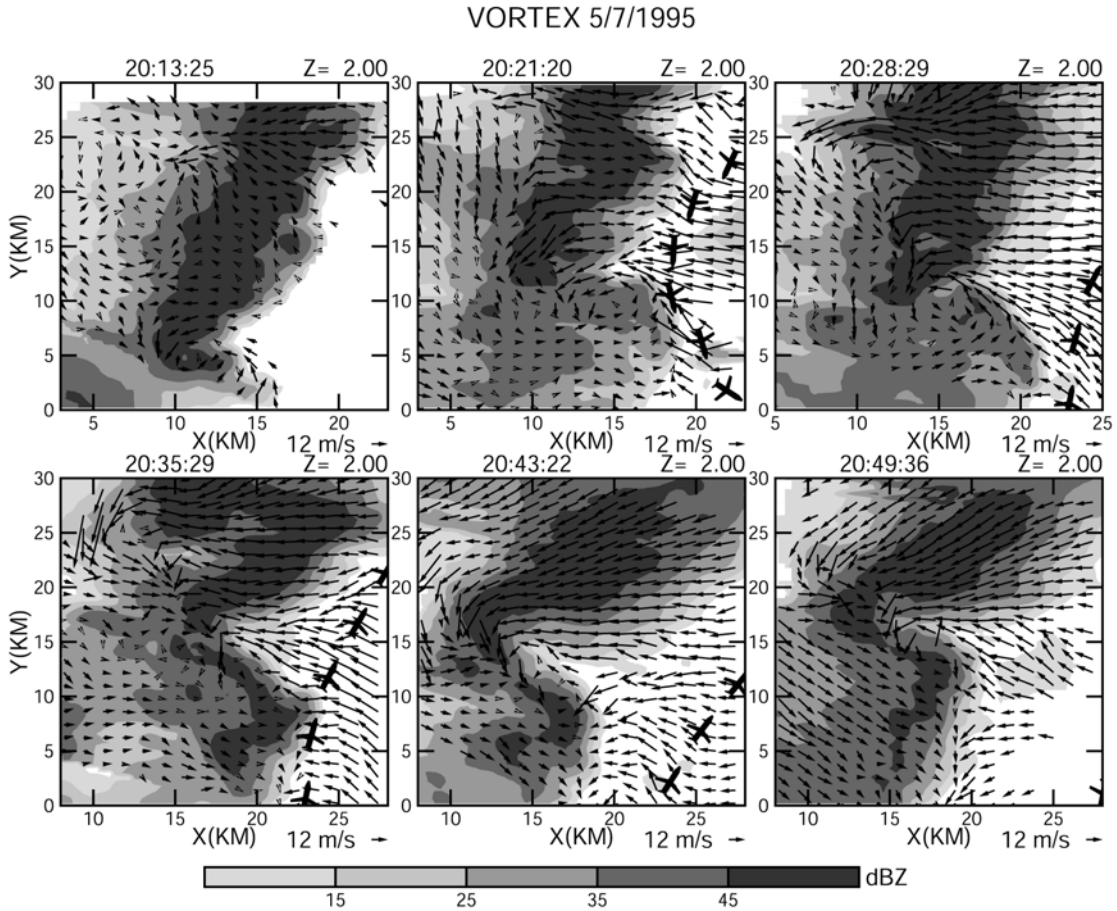

Figure 2: The horizontal cross-sections of the 7 May 1995 squall line at 2 km altitude from 2013 to 2049. The reflectivity is in gray shades and storm-relative winds are in vectors. The aircraft symbols indicate the flight track of the NCAR Electra.

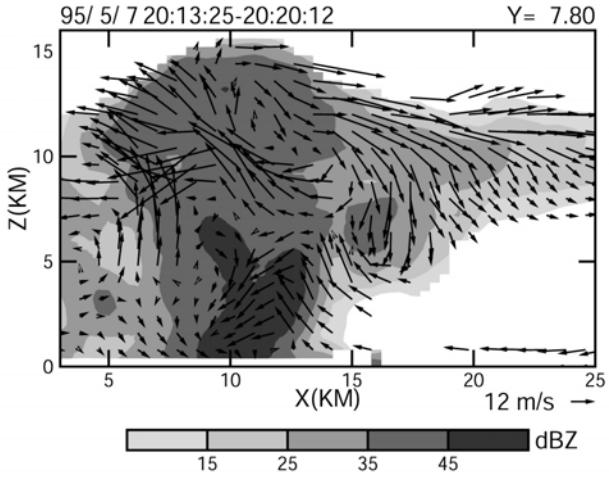

Figure 3: East-west vertical cross-section of the 7 May 1995 squall line at 2013 and y=7.8 km just south of the mesocyclone. Reflectivity is in gray shades and storm-relative winds are in vectors.

3. Summary and future work

This study presents the 7 May 1995 squall line kinematic structures obtained by the NCAR ELDORA via a 3-D variational analysis technique. The structures of this squall line are unique in many aspects that have not been revealed in previous observational studies, such as the vertical velocities in a weak echo vault, the structure of anvil at high incidence angles, 3-D characteristics of a squall line, and the formation of a LEWP.

This study has focused on the evolution of a mesocyclone which is part of a squall line. The vorticity equation will be evaluated using the 3-D wind fields to examine the formation and intensification mechanisms of these mesocyclones and the bow echo as proposed in Lee et al. (1992) and Weisman (1993).

Acknowledgments:

The authors thank Ms. Susan Stringer for producing figures in this paper. This research is partially sponsored by NSF Grant No. 9422499

.

References

Browning, K., and G.B. Foote, 1976: Airflow and hail growth in supercell storms and some implications for hail suppression. Quart. J. Roy. Meteor. Soc., 102, 499-533.

Gamache, J. F., 1997: Evaluation of a fully three-dimensional variational Doppler analysis technique. Preprints, *28th Conf. On Radar Meteorology*, 9-13 Sept. 1997, Austin, AMS.

Lee, W.-C., R. M. Wakimoto, and R. E. Carbone, 1992: The evolution and structure of a "bow-echo-microburst" event. Part II: The bow echo. *Mon. Wea. Rev.,* **120,** 2211-2225.

Oye, R., C. Mueller, and S. Smith, 1995: Software for radar translation, visualization, editing and interpolation. Preprints, *27th Conf. On Radar Meteorology*, 9-13 Sept. 1997, Vail, AMS, 359-363.

Weisman, M. L., 1993: The genesis of severe, long-lived bow echoes. *J. Atmos. Sci.,* **50,** 645-670.

Weisman, M. L., and C. A. Davis, 1998: Mechanisms for the generation of mesoscale vortices within quasi-linear convective systems. *J. Atmos. Sci.*, **55,** 2603-2622.

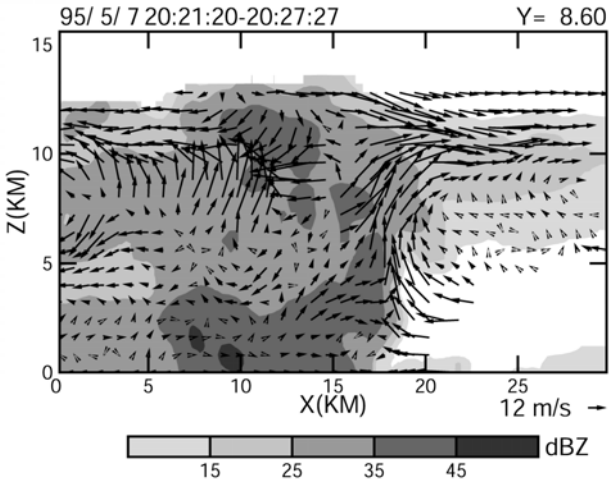

Figure 4: Same as Fig. 3 but for the leg of 2021. The NCAR Electra was located at (18,1) just beneath the weak echo vault.

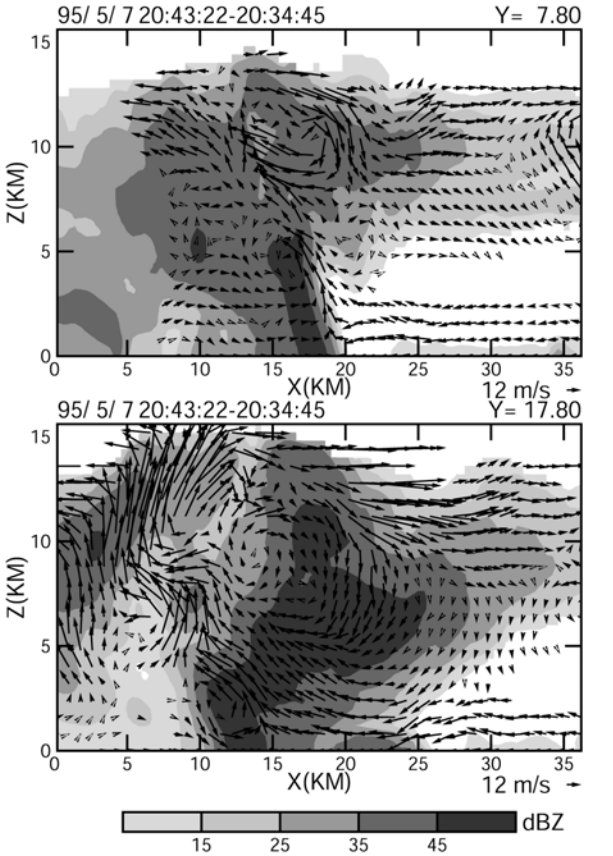

Figure 5: Same as Fig. 4 but for the leg of 2043. Top panel shows the cross-section south of the mesocyclone and the bottom panel shows the cross-section north of the mesocyclone.